Chapter 8

Rapid Detection of Dynamic PTEN Regulation in Living Cells Using Intramolecular BRET

Stanislas Misticone, Evelyne Lima-Fernandes, and Mark G.H. Scott

Abstract

Tumor suppressor PTEN phosphatase acts to inhibit the PI3K/AKT pathway and thus regulates cell proliferation, survival, and migration. Dysregulation of PTEN function is observed in a wide range of cancers. In addition to alterations of the *PTEN* gene, repression of PTEN function can also occur at the protein level through changes in PTEN conformation, localization, activity, and stability. The ability to follow switches in PTEN conformation in live cells provides a rapid approach to study changes in PTEN function and may provide a basis to screen pharmacological agents aimed at enhancing or reestablishing PTEN-dependent signaling pathways that have gone awry in cancer. Here, we describe methods to use an intramolecular bioluminescent resonance energy transfer (BRET)-based biosensor that reports dynamic signal-dependent changes in PTEN conformational rearrangement and function.

Key words PTEN, PI3K/AKT, Tumor suppressor, Phosphatase, Biosensor, Bioluminescence resonance energy transfer, Conformational change, Posttranslational modifications

1 Introduction

Tumor suppressor PTEN (phosphatase and tensin homolog deleted on chromosome ten) is a lipid phosphatase that dephosphorylates phosphatidyl (3, 4, 5) trisphosphate and therefore negatively regulates the pro-survival oncogenic PI3K/AKT pathway. In addition to its role in regulation of the PI3K/AKT pathway, PTEN also displays lipid phosphatase-independent functions including the inhibition of cell migration, regulation of p53 levels and activity, and control of genomic stability [1–4]. While the *PTEN* gene is often targeted by mutation, PTEN function can also be repressed in human cancers at the posttranslational level in the absence of any *PTEN* gene alteration [5]. PTEN is tightly controlled by multiple posttranslational modifications (including phosphorylation, ubiquitination, SUMOylation, and acetylation) and interacting partners that combined regulate PTEN plasticity by

Leonardo Salmena and Vuk Stambolic (eds.), *PTEN: Methods and Protocols*, Methods in Molecular Biology, vol. 1388, DOI 10.1007/978-1-4939-3299-3_8,

impacting conformation, localization, activity, and stability [3, 6, 7]. Perturbation of these different mechanisms can therefore lead to the downregulation of PTEN function in a variety of different ways.

PTEN is comprised of a catalytic domain, a C2 domain, and a C-terminal tail that contains a key regulatory serine-threonine residue cluster [6]. Phosphorylation of these residues by casein kinase 2 (CK2) is thought to promote a "closed" form due to intramolecular interaction of the C-terminal tail with the catalytic and C2 domains of PTEN. This results in enhanced conformational compaction, reduced catalytic activity, and decreased plasma membrane targeting [8–13]. Mutation of the serine-threonine residue cluster in the C-terminal tail disrupts the intramolecular interaction promoting an "open" form of PTEN that displays enhanced activity and plasma membrane targeting. In T-cell acute lymphoblastic leukemia (T-ALL) increased phosphorylation of the serine-threonine cluster in the C-terminal tail leads to the inactivation of PTEN, resulting in enhanced PI3K/AKT signaling [14]. Pharmacological inhibition of CK2 reestablishes PTEN function and inhibits PI3K/AKT signaling in T-ALL cells.

The capacity to monitor PTEN conformation in a direct, rapid, and sensitive manner in live cells is useful to investigate dynamic PTEN regulation. Tools enabling this type of approach may also help form the basis for drug discovery platforms to identify and develop small molecules with the aim of enhancing or reestablishing PTEN-dependent signaling pathways. We recently developed an intramolecular bioluminescence resonance energy transfer (BRET)-based biosensor that is capable of reporting signal-dependent PTEN conformational changes in living cells [15]. In this chapter we provide detailed protocols of how to use the PTEN intramolecular BRET-based biosensor and describe different facets in which it may be employed to investigate cellular regulation.

2 Materials

2.1 Cell Lines

1. Human Embryonic Kidney 293-T (HEK 293 T) cell line.
2. HeLa human cervical cancer cell line.
3. PC-3 human prostate cancer cell line.

2.2 Plasmids

1. BRET plasmids: Rluc-PTEN control vector, Rluc-PTEN-YFP biosensor, Rluc-PTEN-A4-YFP biosensor with Ser380, Thr382, Thr383, and Ser385 phosphorylation sites mutated to alanine [15].
2. Plasmids encoding PTEN regulating proteins: HA-thromboxane A2 receptor (TPαR) and Myc-RhoA-Q63L [15].

2.3 Cell Culture and Transfection

1. Dulbecco's modified Eagle's medium (DMEM), 4.5 g/l glucose, 4 mM glutamine, and 1 mM pyruvate, supplemented with 10 % (v/v) fetal bovine serum, 100 U/ml penicillin, and 0.1 mg/ml streptomycin (Life Technologies).
2. Roswell Park Memorial Institute 1640 Medium (RPMI), GlutaMAX™, 2 g/l glucose, supplemented with 10 % (v/v) fetal bovine serum, 100 U/ml penicillin, and 0.1 mg/ml streptomycin (Life Technologies).
3. Trypsin-EDTA (0.05 %) solution.
4. PBS-EDTA solution: Phosphate-buffered saline (PBS; 1×) without $CaCl_2$ and $MgCl_2$ (Life Technologies) containing 2 mM EDTA.
5. 6- and 12-well plates for cell culture (Falcon, Corning), 96-well sterile white microplates (Perkin Elmer).
6. Poly-L-ornithine (1.5 mg/ml in dH_2O for a 50× stock) used to coat 96-white well plates for adherent cell experiments.
7. Transfection reagents: GeneJuice (Novagen), FuGENE HD Transfection Reagent (Promega).
8. Chemical reagents: U46619 TPαR agonist (Cayman Chemicals), TBB, and CX-4945 CK2 inhibitors (Santa Cruz).

2.4 BRET-Ratio Measurements

1. Coelenterazine-h (Interchim) is dissolved in 100 % ethanol at 2 mM (400× stock solution) and stored at −20 °C in opaque microcentrifuge tubes (*see* **Note 1**).
2. Hanks' balanced salt solution (HBSS; 1×) containing $CaCl_2$ and $MgCl_2$ (Life Technologies).
3. DMEM or RPMI without phenol red.
4. PBS (1×) containing $CaCl_2$ and $MgCl_2$ (Life Technologies).
5. White 96-well plates (Perkin Elmer OptiplateTM-96HB or equivalent) for BRET measurements.
6. Multi-mode microplate reader: Mithras LB 940 (Berthold) or equivalent with BRET 1 filter sets 480 ± 10 nm and 540 ± 20 nm.

3 Methods

3.1 Background

To analyze conformational change of PTEN in live cells, the luminescent BRET-donor (Renilla luciferase, Rluc) is fused to the amino-terminus of PTEN and the fluorescent BRET-acceptor (yellow fluorescent protein, YFP) at the carboxy-terminus, using standard subcloning procedures, to create an Rluc-PTEN-YFP fusion (Fig. 1a and [15]). A control vector encoding Rluc-PTEN and lacking the acceptor YFP is also used to determine the background signal (Fig. 1a). Changes in intramolecular BRET of the Rluc-PTEN-YFP biosensor, depending on the relative orientation

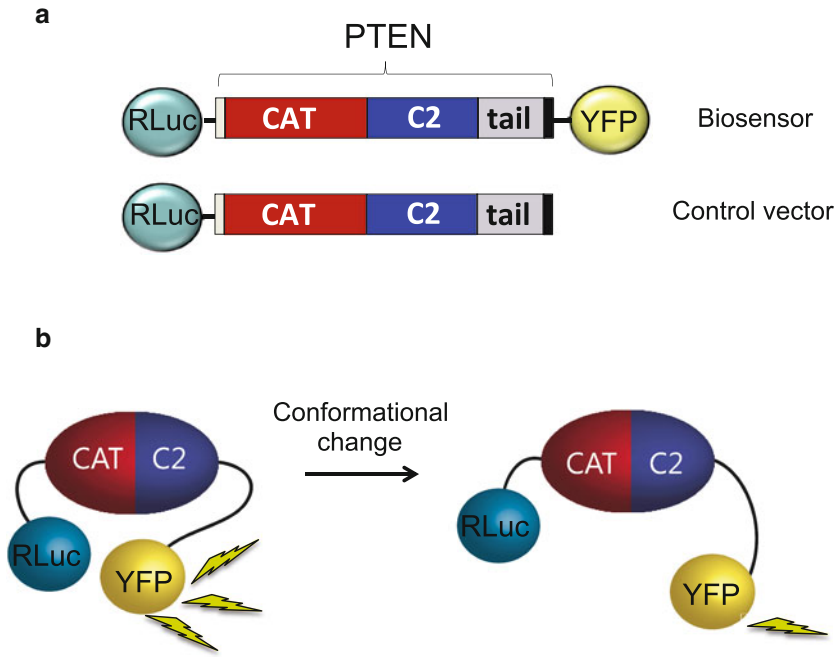

Fig. 1 Schematic representations of the PTEN biosensor. (**a**) Human PTEN is subcloned between Renilla luciferase (Rluc) and yellow fluorescent protein (YFP) to create the genetically encoded Rluc-PTEN-YFP conformational biosensor. An Rluc-PTEN control vector is also used to establish the background BRET signal in the absence of the energy acceptor YFP. (**b**) The diagram depicts how conformational changes in PTEN may induce changes in BRET between Rluc and YFP, although the real orientations of the donor/acceptor pair are not known

of donor and acceptor proteins in the fusion, allow the detection of conformational rearrangement of PTEN in live cells (Fig. 1b). We have previously validated that PTEN within the Rluc-PTEN-YFP fusion maintains functionality: it displays intact lipid phosphatase activity, inhibits cellular pAKT levels, demonstrates expected subcellular localization in live cells, and binds known interaction partners [15]. The Rluc-PTEN-YFP system we describe here is a BRET1 assay but there are now also new-generation BRET2 and BRET3 assays that use modified donor/acceptor pairs (*see* **Note 2**). BRET can be performed in a large variety of intact adherent or suspension mammalian cell lines. For the PTEN biosensor we have tested mouse embryonic fibroblasts, HEK-293 T, HeLa, PC-3, MCF-7, and SKBR3 cell lines. The light emitted by the YFP acceptor over that emitted by the Rluc donor determines the BRET ratio. This is acquired using BRET readers that can perform readings at both wavelengths rapidly and repetitively in wells of 96-well plates. Below, we detail protocols to perform experiments and calculate BRET ratios. In addition we provide details on how to exploit the biosensor to monitor PTEN conformation change in (1) a structure-function mode, (2) experiments using pharmacological inhibitors and PTEN modulators, and (3) real-time kinetics.

3.2 Cell Preparation and Basal BRET Measurements on Adherent Cells

1. 24 h prior to transfection cells are seeded into 6- or 12-well plates to achieve 50–70 % confluence on the day of transfection (*see* **Note 3**). The number of cells seeded per well to achieve this will evidently depend on each cell type, based on cell size and growth rate—in the case of HEK-293 T we seed $100–200 \times 10^3$ cells per well of a 6-well plate in 2 ml of complete DMEM.
2. 24 h after seeding the cells are transfected with 100–200 ng of Rluc-PTEN-YFP or Rluc-PTEN per well of a 6-well plate using either Gene Juice (for HEK 293 T or HeLa cells) or Fugene HD (for PC-3, MCF-7, SKBR3, or MEF cells) according to the manufacturer's instructions. Again the amount transfected should be determined for each new experimental setup.
3. Poly-L-ornithine is used to coat 96-white well plates for adherent cell experiments (*see* **Note 4**). The plates can be prepared in advance and should be incubated for at least 2 h at 37 °C. Prior to cell seeding the plates are washed once with PBS (containing $CaCl_2/MgCl_2$) or complete medium.
4. 24 h post-transfection, cells in each well of the 6-well plate are washed with PBS, detached in either trypsin-EDTA or PBS-EDTA solution at 37 °C, and resuspended in 2 ml of complete medium. The cells are then distributed into the poly-l-ornithine-coated 96-well plates (100 µl per well) and incubated at 37 °C for a further 24 h.
5. The following day, cells are washed with PBS containing $CaCl_2/MgCl_2$. The cells are then overlayed with 90 µl of HBSS or serum-free media without phenol red (*see* **Note 5**) and then 10 µl of a freshly prepared solution of 50 µM coelenterazine-h diluted in HBSS or serum-free media is added to each well giving a final concentration of 5 µM. The samples are then protected from light.
6. After a 3-min incubation at room temperature with coelenterazine-h, BRET readings are initiated using a multi-mode microplate reader that permits sequential integration of light output from Rluc and YFP detected using two filter settings (480 ± 10 nm and 540 ± 20 nm—*see* **Note 6**).

3.3 BRET Measurements on Cells in Suspension

1. Cells are seeded and transfected as described in Subheading 3.2.
2. 24–48 h post-transfection cells are detached from the 6-well plates with PBS-EDTA at 37 °C, transferred to a microcentrifuge tube, and collected by centrifugation at $300 \times g$ for 5 min at room temperature.
3. Cell pellets are resuspended in 500 µl HBSS and 90 µl of the cell suspensions are distributed into wells of a white 96-well plate.
4. As in Subheading 3.2 the BRET measurements are initiated after a 3-min incubation with a freshly prepared coelenterazine solution.

3.4 Calculation of Basal BRET Ratio Obtained with the PTEN Biosensor

The BRET ratio is calculated as the fluorescence signal emitted by YFP (filter 540 ± 20 nm) over the Rluc signal (filter 480 ± 10 nm). Each well is measured for 1 s for each channel and the data (YFP signal, Rluc signal and YFP/Rluc ratio) automatically integrated into BRET reader software (Mikrowin). The wells are read multiple times (generally between three and six times) to generate mean values and the data is exported to a spreadsheet for analysis. Specific BRET ratios (=Net BRET) are then calculated by subtracting the background BRET value, obtained with Rluc-PTEN control vector lacking YFP acceptor, from the mean BRET ratios obtained with Rluc-PTEN-YFP. Values are then converted into mBRET units by multiplying by 1000 to obtain whole numbers, thus circumventing the need to deal with decimal numbers. A spreadsheet with the raw data obtained (Rluc signal, YFP signal, and YFP/Rluc BRET ratio) and the subsequent data analysis in an experiment performed in PC-3 cells is shown in Fig. 2.

3.5 Measuring BRET with Increasing Amounts of PTEN Biosensor

As the donor and acceptor molecule are in the same unimolecular Rluc-PTEN-YFP fusion, the BRET ratio would be predicted to remain stable over a range of different concentrations. An experiment to test this is described below:

1. PC-3 cells are seeded and transfected as described in Subheading 3.2. As different amounts of Rluc-PTEN or Rluc-PTEN-YFP are transfected in this experiment (1–1000 ng) to compare BRET ratios obtained at different expression levels, the total amount of DNA transfected should be completed with "empty" vector such as pcDNA3.1 to the maximal DNA amount.
2. Cells are prepared and BRET measurements initiated as described in Subheading 3.3. BRET ratios obtained can then be plotted against Rluc values (light units) obtained to assess the signal over a range of concentrations (Fig. 3). We have found that the BRET ratio remains stable over a 100-fold range of Rluc values indicating a constant acceptor-to-donor ratio. *See* **Note 7** for evaluating biosensor levels compared to endogenous PTEN.

3.6 Assessing PTEN Conformational Change in a Structure-Function Mode

As mentioned in the introduction, phosphorylation of PTEN on its C-terminal regulatory cluster (Ser 380, Thr 382, Thr 383, Ser 385) promotes a "closed" predominantly cytoplasmic form (Fig. 4a, b). Dephosphorylation of these residues favors an "open" form of PTEN that displays increased plasma membrane targeting (Fig. 4a–d). The biosensor can be used in a structure-function mode to determine whether mutation of amino acids results in conformational change. An experiment to test this is described below:

1. Cells (HEK-293 T, PC-3, or HeLa) are seeded and transfected as described in Subheading 3.2 with either WT Rluc-PTEN-

a

	Rluc-PTEN				Rluc-PTEN-YFP			
Rluc Signal	Well A1	Well B1	Well C1	Well D1	Well E1	Well F1	Well G1	Well H1
Reading 1	111587	121883	118100	121157	120569	121317	123728	124301
Reading 2	107663	116766	114005	116789	117573	117386	121061	119960
Reading 3	102219	111930	109169	110776	113222	113912	116579	115128
Reading 4	97484	107383	104879	106298	108740	108915	111969	109712
YFP Signal								
Reading 5	81962	89006	86580	89443	124664	125834	127811	128525
Reading 6	78429	85379	83125	85067	121844	121914	125436	124067
Reading 7	75005	82212	79622	81674	118205	118697	121142	118638
Reading 8	71659	78546	76963	78156	112449	114380	116228	113934
BRET ratio								
Reading 9	0.7345	0.7303	0.7331	0.7382	1.0340	1.0372	1.0330	1.0340
Reading 10	0.7285	0.7312	0.7291	0.7284	1.0363	1.0386	1.0361	1.0342
Reading 11	0.7338	0.7345	0.7293	0.7373	1.0440	1.0420	1.0391	1.0305
Reading 12	0.7351	0.7315	0.7338	0.7353	1.0341	1.0502	1.0380	1.0385
Mean BRET ratio	0.7330	0.7319	0.7314	0.7348	1.0371	1.0420	1.0366	1.0343
Background BRET ratio			0.7327					
Specific BRET ratio					0.3044	0.3093	0.3038	0.3016
Specific mBRET					304.4	309.3	303.8	301.6
Mean Specific mBRET						305		

b

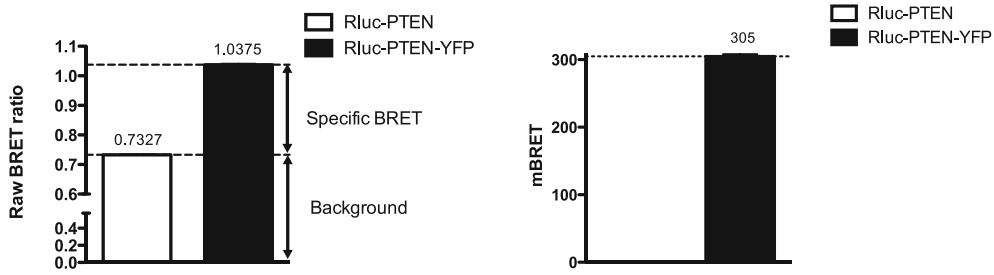

Fig. 2 Calculation of specific BRET ratio and mBRET values obtained with the PTEN biosensor in PC-3 cells. (**a**) Raw BRET data acquisition and analysis. PC-3 cells growing in 6-well plates were transfected with either Rluc-PTEN control vector or Rluc-PTEN-YFP (3-wells transfected for each construct). Cells from each transfection were distributed into four wells of a white 96-well plate and BRET ratios measured four times each for each well. For simplicity, only readings from cells from one 6-well for each construct split into four 96-wells are shown. Wells A1–D1 represent readings obtained from Rluc-PTEN and wells E1–H1 represent those obtained with Rluc-PTEN-YFP. The Rluc values obtained are shown in the Rluc signal rows (Readings 1–4), and those for YFP values in the YFP signal rows (Readings 5–8). The BRET values are shown in the BRET ratio rows (Readings 9–12). The mean BRET ratio is calculated from rows 9–12 and the background determined from the average of these values in wells A1–D1 expressing Rluc-PTEN donor only. Specific BRET ratios are then calculated by subtracting the background BRET value from the mean BRET ratios obtained with Rluc-PTEN-YFP in wells E1–H1. These values are then multiplied by 1000 to obtain mBRET units to circumvent the need to deal with decimal numbers. (**b**) The raw BRET measurements are shown in the *left panel* indicating the background BRET obtained with Rluc-PTEN (*white bar*) and the specific net BRET obtained with Rluc-PTEN-YFP (*filled bar*). The *right panel* shows the specific mBRET values obtained with Rluc-PTEN-YFP (305 mBRET) with Rluc-PTEN being set to 0 mBRET

YFP or the mutant PTEN biosensor Rluc-PTEN(A4)-YFP that has the phosphorylation cluster serine/threonine residues mutated to alanine.

2. 24–48 h after transfection, cells are prepared and BRET measurements initiated as described in Subheading 3.3. BRET measurements are shown for HEK cells in Fig. 4e–g. Figure 4e shows the mBRET units obtained with the WT and A4 biosensor. There was a marked reduction in the BRET signal obtained with the A4 form of PTEN compared to WT PTEN, indicating conformational change. The data can be expressed as ΔmBRET versus the WT PTEN biosensor, which is therefore set to zero, and the change obtained with the mutant is expressed relative to this (Fig. 4f). The data can also be represented as %ΔmBRET where the change is represented as a percentage difference compared to that obtained with WT sig-

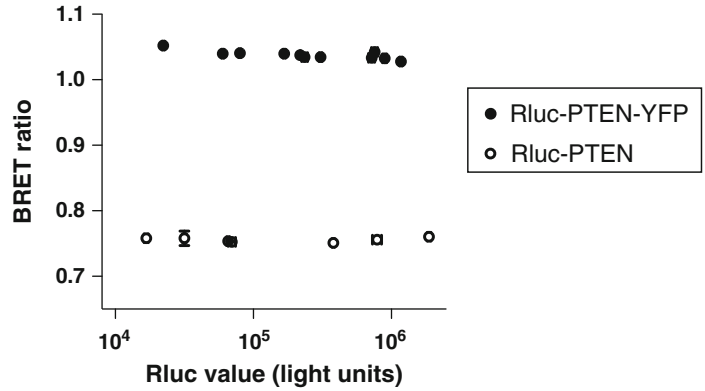

Fig. 3 Stable intramolecular BRET obtained with increasing amounts of PTEN biosensor. PC-3 cells growing in 6-well plates were transfected with increasing amounts of either Rluc-PTEN control vector or Rluc-PTEN-YFP (1–1000 ng). Twenty-four hours later, cells from each transfection were distributed into four wells of a white 96-well plate and BRET ratios measured. The BRET signal is constant over a 100-fold range of Rluc light values due to the constant acceptor-to-donor ratio in the unimolecular biosensor

Fig. 4 (continued) antibody that recognizes phospho-PTEN (Ser380/Thr382/Thr383) in addition to total PTEN expression. (**d**) Live HEK cells expressing WT or A4 forms of PTEN biosensor were directly imaged in IBIDI μ-slide multi-well dishes (Biovalley). The *insets* show magnified regions of the *boxed area* and demonstrate membrane-targeting of PTEN-A4. Scale bar is 10 μm. (**e**) BRET values obtained with the WT and A4 forms of PTEN biosensor in HEK cells, expressed as mBRET. (**f**) The BRET values obtained in (**e**) are expressed as ΔmBRET to show the shift in BRET compared to WT signal, which is set to zero. (**g**) The BRET values obtained in (**e**) can also be expressed as the % change compared to WT signal (Δ%mBRET). (**h**) Δ%mBRET change obtained with the A4 PTEN biosensor in PC-3 cells. (**i**) Δ%mBRET change obtained with the A4 PTEN biosensor in HeLa cells

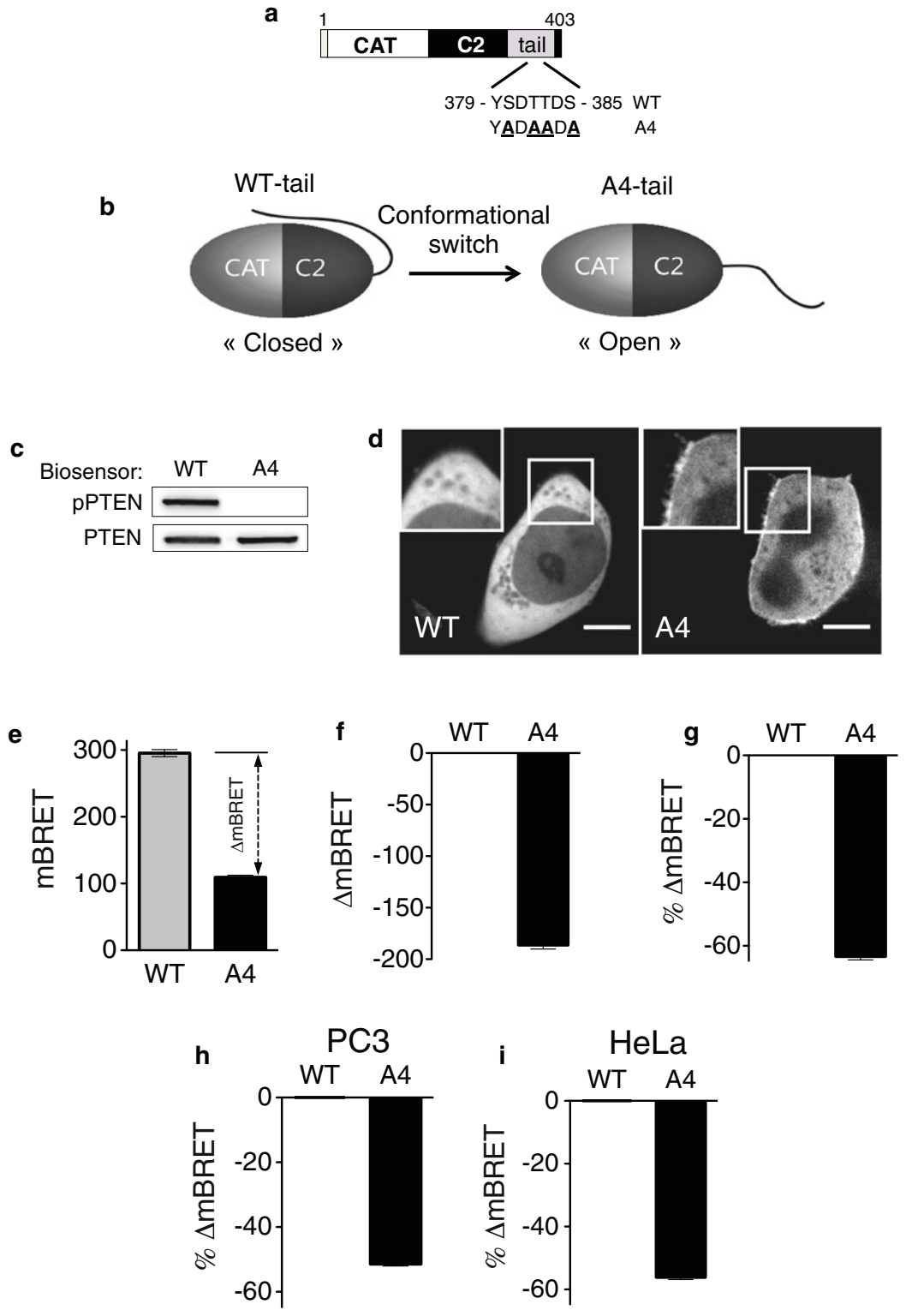

Fig. 4 Detection of PTEN conformational change in live cells following mutation of key regulatory residues in the C-terminal tail. (**a**) Diagram showing key regulatory phosphorylation sites in the C-terminal tail of PTEN at Ser380, Thr382, Thr383, and Ser385. The A4 mutant has all of these phosphorylation sites mutated to alanine. (**b**) Proposed model of the conformational switch that occurs in the A4 form of PTEN. (**c**) A western blot with an

nal (Fig. 4g). Similar data were obtained using PC-3 (Fig. 4h) and HeLa (Fig. 4i) cells. Following changes in BRET signal, secondary tests can be performed to assess potential functional changes (*see* **Note 8**). While these functional tests can be applied to the structure-function mode they are evidently also applicable to the other experimental modes in which the biosensor can be used, described below in Subheadings 3.7–3.9.

3.7 Assessing PTEN Conformational Change by Pharmacological Inhibitors That Impact PTEN Phosphorylation

CK2 overexpression has been documented in different types of cancer and CK2 inhibitors have been developed for clinical use [16, 17]. CK2 is implicated in the phosphorylation of the C-terminal regulatory phosphorylation cluster of PTEN. This leads to phospho-dependent inhibition of PTEN and increased activation of the PI3K/AKT pathway. CK2 inhibitors have been shown to reestablish PTEN signaling and restrain the PI3K/AKT pathway. The experiment described below demonstrates how the PTEN biosensor can be used to report changes in its phosphorylation status in the presence of pharmacological inhibitors.

1. PC-3 cells are seeded and transfected as described in Subheading 3.2.
2. 48 h after transfection cells are treated with the CK2 inhibitors tetrabromobenzotriazole (TBB; 50 μM) or CX-4945 (10 μM) for 2 h (0.1 % DMSO is used as vehicle control). The cells are then prepared for BRET readings as described in either Subheading 3.2 or 3.3. To ensure that pharmacological agents do not affect the spectral properties of YFP, raw YFP measurements can be taken in the presence of vehicle or pharmacological agent (*see* **Note 9**). In this experiment the PTEN phosphorylation status can be assessed in parallel by subsequent western blotting using an anti-phospho Ser380/Thr382/Thr383 antibody (Cell Signaling). Both CK2 inhibitors induce a decrease in BRET signal (Fig. 5). The effect was more pronounced with CX-4945 and this was associated with a greater decrease in phospho Ser380/Thr382/Thr383 compared to that obtained with TBB (Fig. 5).

3.8 Assessing PTEN Conformational Change by Cellular PTEN Regulators

The biosensor can also be used to test the effect of PTEN regulators on conformation. For this the PTEN partner/regulator is simply co-expressed with the biosensor. The experiment described below uses an active form of RhoA (RhoA-Q63L) known to increase PTEN activity.

1. HEK 293 T cells are seeded and transfected as described in Subheading 3.2 with 5 ng biosensor and either 250 ng empty Myc-RK5 vector or Myc-RhoA-Q63L (*see* **Note 10** for DNA ratios of partner/regulator to biosensor).
2. The cells are then prepared for BRET readings as described in Subheading 3.3. In this experiment the levels of cellular pAKT

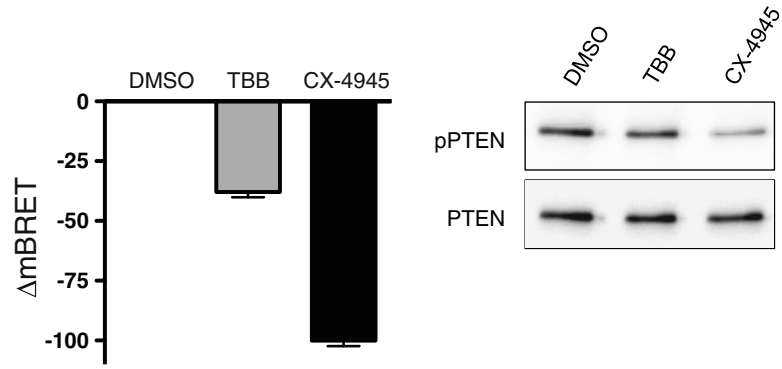

Fig. 5 Detection of PTEN conformational change in live cells following pharmacological modulation of PTEN regulatory pathways. (**a**) ΔmBRET values obtained following a 2-h incubation with the CK2 inhibitors TBB (50 μM) or CX-4945 (10 μM) versus DMSO vehicle control in PC-3 cells expressing WT PTEN biosensor. (**b**) Western blot showing phosphorylation of the Ser380/Thr382/Thr383 cluster in the presence of DMSO, TBB, or CX-4945 in PC-3 cells expressing WT PTEN biosensor

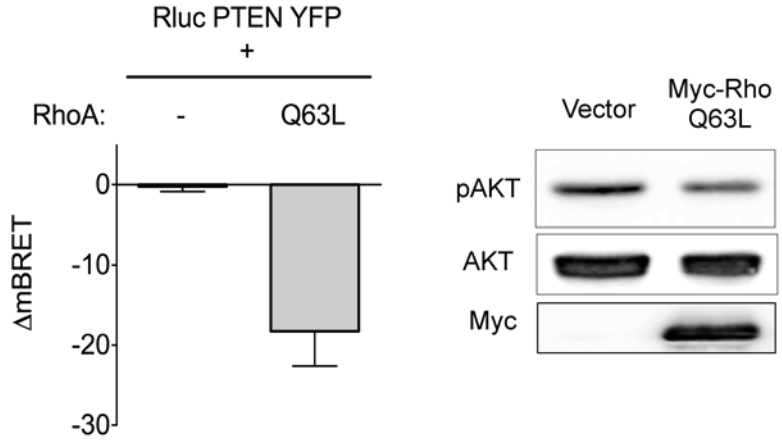

Fig. 6 Detection of signal-dependent PTEN conformational change in live cells. (**a**) ΔmBRET values obtained with the WT PTEN biosensor in HEK cells transfected with either empty vector or Myc-RhoA-Q63L. (**b**) HEK cells transfected with empty vector or RhoA-Q63L were assessed for pAKT levels by western blotting

can be assessed in parallel by subsequent western blotting using an anti-phospho Ser 473 antibody (Cell Signaling). Active RhoA-Q63L induces a decrease in BRET signal and this is associated with a decrease in pAKT levels (Fig. 6).

3.9 Assessing Real-Time Changes in PTEN Conformation Following Cell Surface Receptor Activation

BRET can also be used to follow conformational change of PTEN in real time in living cells. For technical reasons the length of these experiments when using coelenterazine-h is limited to around 20 min (*see* **Note 11**). The experiment described below uses the G protein-coupled receptor, TPαR, which activates PTEN [15, 18].

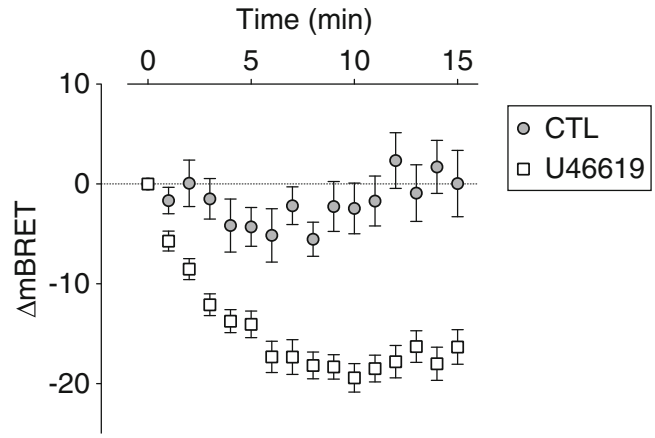

Fig. 7 Real-time analysis of cell surface receptor-induced PTEN conformational change in live cells. Changes in BRET induced by addition of the agonist U46619 for the TPαR. Cells were co-transfected with TPαR and biosensor, and subsequently transferred to poly-L-ornithine-coated plates. BRET readings were acquired every minute after addition of 1 μM U46619 or vehicle control (0.03 % methyl acetate) over a period of 15 min

1. HEK 293 T cells are seeded and transfected as described in Subheading 3.2 with 5 ng biosensor and 250 ng of the TPαR. *See* **Note 10** for DNA ratios of partner/regulator to biosensor.
2. The cells growing in poly-L-ornithine-coated 96-well white plates are serum-starved overnight and then the media is replaced with 80 μl DMEM without phenol red per well. 10 μl of a freshly prepared solution of coelenterazine-h diluted in serum-free media is added to each well, and then 10 μl of an appropriate intermediate stock solution of U46619 or of methyl acetate (vehicle control) is added to each well.
3. BRET readings are then immediately initiated and repeated over the course of the experiment to observe the evolution over time. The BRET ratios obtained are then plotted against time as shown in Fig. 7.

4 Notes

1. Coelenterazine-h is sensitive to light and undergoes slow oxidation. Working solutions are prepared at 50 μM in HBSS or in media without phenol red, immediately before performing experiments. Coelenterazine-h should be protected from light during prolonged storage periods by using opaque tubes. The experiments described here with the PTEN biosensor in a BRET1 assay employed coelenterazine-h as substrate. Other

Rluc substrates are available to obtain either increased luminescence (three- to fivefold increase in peak signal with ViviRen™ from Promega) or extremely stable luminescence over a 24-h period (but with 10–25 times lower signal) using EnduRen™ (Promega). To reduce degradation rates, both of these substrates carry protecting groups that are cleaved by esterases inside cells.

2. Changes in donor and acceptor pairs, as well as different substrates, can be used to generate increased sensitivity BRET1, BRET2, or BRET3 assays. BRET 1 is still the most widely performed assay using Rluc as the energy donor and the enhanced yellow fluorescent protein (YFP) as acceptor. Rluc variants, such as Rluc8, and the YFP variant YPet have been developed that demonstrate increased BRET signals using this BRET couple compared to the standard Rluc/YFP pair. A luciferase subunit (MW: 19 kDa) from the deep sea shrimp *Oplophorus gracilirostris* was recently described and developed by Promega. This new luciferase, Nanoluc™, uses furimazine as substrate and displays around 150-fold greater specific activity than Rluc. The maximal emission peak of Nanoluc™ is 465 nm and it is therefore compatible as donor in BRET1 assays. The increased brightness obtained with Nanoluc™ allows very low expression levels and it is therefore ideally adapted to monitoring protein fusions at "endogenous" cellular levels. BRET2 assays use the substrate coelenterazine 400a with a modified form of Rluc donor called Rluc2, and GFP2, a GFP mutant that can be excited at 400 nm, as the energy acceptor. BRET2 provides the advantage of demonstrating increased spectral resolution between donor and acceptor peaks and therefore displays lower background signal. Incubation of Rluc2 with coelenterazine 400a causes Rluc2 to emit light at 400 nm, promoting the excitation of GFP2, which, subsequently, emits light at 510 nm. Filter sets used for BRET2 are 400 ± 10 nm and 515 ± 10 nm. BRET3 assays use coelenterazine-h with Rluc8 as donor and mOrange (a mutant form of DsRed2) as acceptor that can be excited from 514 to 550 nm and that has maximal emission at 564 nm. This is therefore the BRET configuration that gives the most red-shifted light output.
3. BRET assays should be performed on "fresh" cells that have not been in culture for more than 6 weeks. Routine testing for mycoplasma (e.g., MycoAlert™ Mycoplasma Detection Kit, Lonza) should also be carried out to ensure that cells are free of contamination.
4. Poly-L-ornithine used to coat plates is prepared in 1 ml aliquots at a concentration of 1.5 mg/ml (50×) in sterile dH_2O. Five 96-well plates can therefore be coated at a time using one 50×

aliquot diluted to 1× in dH_2O (100 µl/well of 30 µg/ml poly-L-ornithine) and the plates can be kept at 37 °C for up to a week before use. Prior to cell seeding, the poly-L-ornithine is removed, wells washed once in PBS (containing $CaCl_2$/$MgCl_2$) or complete medium, which is then also removed, and the wells left to air-dry under the hood.

5. When performing BRET on attached cells, the media should be removed by washing once with PBS (containing $CaCl_2$/$MgCl_2$) to remove phenol red, as this quenches luciferase signal.
6. Previously characterized optimal BRET1 filter sets used in the experiments described here are 480 ± 10 nm and 540 ± 20 nm, which were found to provide enhanced BRET readings compared to 485 + 10 nm and 530 ± 12.5 nm filter sets [19].
7. To measure BRET at "physiological" levels of biosensor expression, cells can be transfected with a range of plasmid concentrations, subsequently lysed, and assessed by western blotting with an anti-PTEN antibody (Cell Signaling or Cascade). The level of biosensor can be compared to endogenous PTEN in the same cells or in comparison with a PTEN-expressing line if the cells used for the BRET study are PTEN-null [15]. When decreasing the amount of biosensor it is important to check that the Rluc and YFP stay in the linear range of detection of the BRET reader.
8. Following changes in BRET signal, secondary tests can be performed to assess potential functional changes. The YFP in the fusion enables direct visualization of PTEN subcellular localization in live cells using fluorescence microscopy. We have found that setting cells up in parallel in IBIDI µ-slide multiwell dishes (Biovalley) provides a convenient way to directly visualize PTEN under multiple test conditions (Fig. 4d). Following cell lysis, the biosensor can also be immunoprecipitated using an anti-GFP antibody (Roche) and phosphatase activity against PI(3,4,5)P3 tested in vitro. The same lysates can also be assessed for changes in cellular pAKT levels.
9. Control readings can be performed in experiments using pharmacological agents to check that raw YFP emissions are not altered, which could indirectly affect BRET. This is done simply by measuring the raw fluorescence emitted at 535 nm by Rluc-PTEN-YFP following external excitation at 485 nm on samples exposed to either vehicle or test reagent [15]. Rluc-PTEN is used to assess background fluorescence from the cells.
10. When assessing the effect of a protein partner/regulator or cell surface receptor on PTEN conformation we have found that DNA ratios of test protein:biosensor of 10:1 to 50:1 work best [15]. Using this approach we have shown the expression of CK2 causes an increase in BRET signal and that expression of

β-arrestin 2 promotes a decrease in BRET, as with active RhoA [15]. A subset of partners that bind PTEN via its C-terminal PDZ-binding sequence may not lend themselves to this approach due to the C-terminal fusion of YFP in the biosensor.

11. As Rluc light output declines with time, kinetic experiments using real-time measurements are limited to a time frame of around 20–25 min. For experiments investigating longer time points "reverse kinetics" can be set up, stimulating cells for the longest time point first and then working down to t = 0 min, when all time points can be measured simultaneously for BRET. Alternatively, Enduren™ substrate that provides stable luminescence over long time periods (*see* **Note 1**) could be used.

Acknowledgements

We thank J. Paradis and C. Boularan for critical reading of the manuscript. This work was supported by the Fondation ARC pour la Recherche sur le Cancer, Ligue Contre le Cancer (comité de l'Oise), Fondation pour la Recherche Biomedicale ("Equipe FRM"), CNRS, and INSERM. The laboratory is part of the multidisciplinary "Who am I?" LABEX and S.M. is supported by a LABEX doctoral fellowship. E.L.F. was funded by a doctoral fellowship from the Fondation ARC pour la Recherche sur le Cancer and subsequently a postdoctoral fellowship from the Fondation Nationale pour la Recherche Luxembourg and Marie Curie Actions.

References

1. Salmena L, Carracedo A, Pandolfi PP (2008) Tenets of PTEN tumor suppression. Cell 133(3):403–414
2. Song MS, Salmena L, Pandolfi PP (2012) The functions and regulation of the PTEN tumour suppressor. Nat Rev Mol Cell Biol 13(5): 283–296
3. Worby CA, Dixon JE (2014) PTEN. Ann Rev Biochem 83:641–669
4. Lima-Fernandes E, Enslen H, Camand E, Kotelevets L, Boularan C, Achour L, Benmerah A, Gibson LC, Baillie GS, Pitcher JA, Chastre E, Etienne-Manneville S, Marullo S, Scott MG (2011) Distinct functional outputs of PTEN signalling are controlled by dynamic association with beta-arrestins. EMBO J 30(13): 2557–2568
5. Leslie NR, Foti M (2011) Non-genomic loss of PTEN function in cancer: not in my genes. Trends Pharmacol Sci 32(3):131–140
6. Hopkins BD, Hodakoski C, Barrows D, Mense SM, Parsons RE (2014) PTEN function: the long and the short of it. Trends Biochem Sci 39(4):183–190
7. Naguib A, Trotman LC (2013) PTEN plasticity: how the taming of a lethal gene can go too far. Trends Cell Biol 23(8):374–379
8. Torres J, Pulido R (2001) The tumor suppressor PTEN is phosphorylated by the protein kinase CK2 at its C terminus. Implications for PTEN stability to proteasome-mediated degradation. J Biol Chem 276(2):993–998
9. Vazquez F, Ramaswamy S, Nakamura N, Sellers WR (2000) Phosphorylation of the PTEN tail regulates protein stability and function. Mol Cell Biol 20(14):5010–5018
10. Rahdar M, Inoue T, Meyer T, Zhang J, Vazquez F, Devreotes PN (2009) A phosphorylation-dependent intramolecular interaction regulates the membrane association and activity of the

tumor suppressor PTEN. Proc Natl Acad Sci U S A 106(2):480–485

11. Das S, Dixon JE, Cho W (2003) Membrane-binding and activation mechanism of PTEN. Proc Natl Acad Sci U S A 100(13):7491–7496
12. Bolduc D, Rahdar M, Tu-Sekine B, Sivakumaren SC, Raben D, Amzel LM, Devreotes P, Gabelli SB, Cole P (2013) Phosphorylation-mediated PTEN conformational closure and deactivation revealed with protein semisynthesis. Elife 2:e00691
13. Odriozola L, Singh G, Hoang T, Chan AM (2007) Regulation of PTEN activity by its carboxyl-terminal autoinhibitory domain. J Biol Chem 282(32):23306–23315
14. Silva A, Yunes JA, Cardoso BA, Martins LR, Jotta PY, Abecasis M, Nowill AE, Leslie NR, Cardoso AA, Barata JT (2008) PTEN post-translational inactivation and hyperactivation of the PI3K/Akt pathway sustain primary T cell leukemia viability. J Clin Invest 118(11): 3762–3774
15. Lima-Fernandes E, Misticone S, Boularan C, Paradis JS, Enslen H, Roux PP, Bouvier M, Baillie GS, Marullo S, Scott MG (2014) A biosensor to monitor dynamic regulation and function of tumour suppressor PTEN in living cells. Nat Commun 5:4431
16. Barata JT (2011) The impact of PTEN regulation by CK2 on PI3K-dependent signaling and leukemia cell survival. Adv Enzyme Regul 51(1):37–49
17. Martins LR, Lucio P, Melao A, Antunes I, Cardoso BA, Stansfield R, Bertilaccio MT, Ghia P, Drygin D, Silva MG, Barata JT (2014) Activity of the clinical-stage CK2-specific inhibitor CX-4945 against chronic lymphocytic leukemia. Leukemia 28(1):179–182
18. Song P, Zhang M, Wang S, Xu J, Choi HC, Zou MH (2009) Thromboxane A2 receptor activates a Rho-associated kinase/LKB1/PTEN pathway to attenuate endothelium insulin signaling. J Biol Chem 284(25): 17120–17128
19. Achour L, Kamal M, Jockers R, Marullo S (2011) Using quantitative BRET to assess G protein-coupled receptor homo- and heterodimerization. Methods Mol Biol 756:183–200